Materials and Design 164 (2019) 107563

Contents lists available at ScienceDirect

Materials and Design

journal homepage: www.elsevier.com/locate/matdes

A critical assessment of the effect of indentation spacing on the measurement of hardness and modulus using instrumented indentation testing

P. Sudharshan Phani [a,*], W.C. Oliver [b]

[a] International Advanced Research Centre for Powder Metallurgy & New Materials (ARCI), Balapur P.O., Hyderabad, Telangana 500005, India
[b] Nanomechanics Inc., 105 Meco Ln, Oak Ridge, TN 37830, USA

HIGHLIGHTS

- Minimum indent spacing can be 10 times the indentation depth for a Berkovich tip, as against the current standard of 20
- Full 3D finite element analysis of sequential indentation for visualization of plastic zones in 2D indentation arrays
- Rationalization of the new spacing criteria based on a strength approach in contrast to well accepted strain approach
- Enhancement of resolution limit of nanoindentation mapping
- High resolution mapping enables coupling with microstructure-based modeling within an ICME approach

GRAPHICAL ABSTRACT

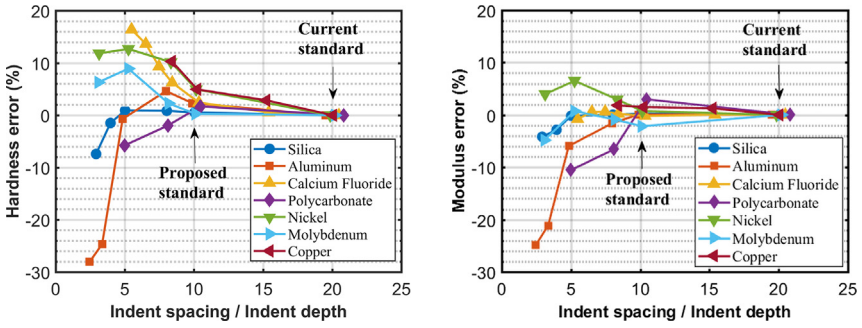

ARTICLE INFO

Article history:
Received 21 November 2018
Received in revised form 19 December 2018
Accepted 20 December 2018
Available online 21 December 2018

Keywords:
Hardness
Elastic property
Finite element analysis
Nanoindentation
Mapping

ABSTRACT

With the advances in instrumented indentation systems and testing methodologies, high speed indentation mapping with indents that take less than a second is now possible. This can be gainfully used to measure the local mechanical properties of multi-phase alloys and small volumes of materials with high throughput, which brings into question the minimum spacing between indents required to prevent interactions from neighboring indents. In this study, extensive indentation experiments (~50,000) and finite element simulations are carried out for a wide range of materials to systematically determine the minimum spacing of indents. It was found that a minimum indent spacing of 10 times the indentation depth is sufficient to obtain accurate results for a Berkovich indenter. This is less than half of the commonly followed criteria of spacing the indents three times the lateral dimension (or 20 times the depth). Similar results were also found for other indenter geometries. It was found that non-overlapping plastic zones are not a requirement for determining the minimum indent spacing and the new criteria is rationalized by simple energy arguments. These results significantly enhance the capabilities of indentation mapping technique which is recently being used as a critical characterization tool for accelerating materials development.

1. Introduction

Indentation based techniques have been widely used to measure the mechanical properties of materials and specifically, indentation hardness

* Corresponding author.
E-mail address: spphani@arci.res.in (P. Sudharshan Phani).

https://doi.org/10.1016/j.matdes.2018.107563

is a widely used measure of plastic response of materials [1]. While the different hardness techniques commonly used differ in test setup, tip geometry, test methodology etc., they all essentially involve applying a known amount of load and determining the area of the residual indent either directly as in conventional hardness testing [1] or through measurement of depth as in instrumented indentation [2]. One of the important parameters for any indentation test apart from selection of load and indenter geometry, is spacing of indents. While this is not very critical for testing on bulk materials where usually there is a lot of measurable area and the neighboring indents can be conveniently spaced much farther, it is extremely important for measuring the properties of small volumes of materials, where local variations in mechanical properties is of prime interest. Such studies are been increasingly carried out using instrumented indentation in recent times [3–7]. However, as the size of microstructural features decreases, indentation depth and thereby indent size has to be reduced in order to accommodate multiple indents within the feature of interest for a given spacing of indents, which may not be feasible beyond a certain level as the precision and accuracy of the indentation tests results can significantly reduce at smaller depths. The minimum indentation depth to achieve reliable results is usually determined by the testing instrument, test methodology and the test conditions which many users may not have much control on. In this scenario, the other alternative is to reduce the indent spacing, which brings into question the minimum indent spacing of indents. Samuels and Mulhearn [8] suggested a minimum spacing of three times the lateral dimension of the indent in a work that goes back several decades and is still being followed in various indentation testing standards [9–14]. The commonly followed criteria for indent spacing [8], has been formulated based on the concept of spacing the indents such that the plastic strain zones underneath the indent do not overlap and hence may not necessarily indicate the absolute minimum spacing for performing indentation. It is worth noting that the minimum spacing criteria is only applicable for indentation tests that cause a permanent impression and not for indents that recover completely as in the case of perfectly elastic deformation, in which case they can be placed as close as desired.

With the latest advances in instrumented indentation, tests can now be performed with a high degree of precision even for indentations depths as small as 50 nm. In addition, the advances in electronics have also enabled fast measurements without compromising the accuracy or noise [15]. High speed nanoindentation testing not only opens up a significant opportunity to measure the local mechanical properties by large arrays of indents [7], but also serve as an effective characterization tool to significantly reduce design and production time [3]. This further emphasizes the need to systematically determine the minimum spacing of indents to accurately capture the local variations in mechanical properties.

In the present work, we critically assess the minimum indent spacing by performing extensive indentation testing over a range of spacings for a wide variety of bulk materials and one coating system to determine the minimum spacing at which deviation in hardness or modulus is insignificant. Full 3D finite element analysis (FEA) of sequential indentation for different indent spacings, is also performed to visualize the plastic zones underneath the indent in order to rationalize the experimental observations. The results indicate that the minimum required spacing of indents is significantly less than the well accepted criteria of 3 times the indent diameter [8]. In addition to the indent spacing effect, the effect of indenter angle, indenter orientation and the number of neighboring indents is also studied to enable broader understanding of the spacing effect.

2. Materials and methods

2.1. Experimental details

One of the main objectives of the current work is to perform extensive indentation tests on a wide range of materials at different indent spacings. In order to achieve this objective within a reasonable amount of time, a high speed nanoindentation technique called NanoBlitz3D was used on an iNano® nanoindenter with an InForce50 actuator (Nanomechanics Inc., Oak Ridge, USA), wherein, a single indentation test, including positioning the sample at the appropriate location, surface approach, loading and unloading takes less than 1 s. Except for the duration of testing, this technique is similar to a standard static indentation test performed using a nanoindenter. The test outputs are similar to any standard nanoindentation test i.e., load, depth, stiffness at maximum load, which are in turn used to calculate the hardness and elastic modulus using the standard Oliver-Pharr approach [2] at the applied maximum load or depth. Indentation arrays of 35×35 (1225 indents) were performed to maximum depths ranging from 600 nm to 1000 nm depending on the material for a given spacing. Tests were performed at normalized spacing, defined as the ratio of indent spacing (d) to the maximum indentation depth (h), of 5, 8, 10, 15 and 20. In order to cover a wide variety of materials, tests were performed on fused silica, annealed pure aluminum, single crystal copper, polycarbonate, calcium fluoride, nickel and molybdenum. In order to assess the applicability of the results to film on substrate systems, a gold film on silica substrate, which being a soft film on hard substrate, represents an extreme case where considerable pile-up is expected, is also tested. In all, 6125 tests were performed on each material and close to 50,000 indents across materials, to draw statistically significant conclusions from the experimental results. In addition to indentation tests, the high-speed mapping technique was also used to map the topography of the residual impression for select cases. The topographic mapping was carried out by detecting the surface at discrete points in the region of interest with a detection threshold of 50 μN and has a sub-nanometer depth resolution and 300 nm lateral resolution.

2.2. Finite element analysis (FEA)

Full 3D FEA is used to simulate indentation arrays at a given spacing in order to study the effect of spacing and also the effect of orientation and number of neighboring indents. Majority of the arrays involve 2 indents at the chosen spacing performed one after the other as a single simulation. The simulations are performed using a commercial FEA package ABAQUS 6.9. A three-sided pyramidal indenter geometry was chosen as it is most commonly used for nanoindentation. The 6-fold symmetry of the 3-sided pyramid could not be used to reduce the computational time as the present work involves simulating indentation arrays for which such symmetry boundary conditions do not apply. Three different indenter geometries are used to study the effect of indenter angle on the minimum spacing of indents. While the standard Berkovich geometry with centerline to face angle of 65.3° was used for majority of simulations, a few simulations were also performed with indenters of centerline to face angle of 55 and 45°. Similar to the experiments, indentation simulations were carried out to different spacings, at a fixed depth, to obtain different normalized spacings (indent spacing/depth) of 3, 5, 8, 10 and 20.

Eight-node linear hexahedral elements (C3D8R) with reduced integration were used to mesh the model as shown in Fig. 1. The model had 76,037 elements. In order to capture the deformation behavior more accurately as well as to reduce the simulation time, finer mesh was used close to the contact region as shown in the figure and a few wedge and tetrahedral elements were used in the mesh transition region further away from the contact. The overall dimensions of the model were chosen such that the edge effects were negligible. Mesh convergence studies were performed to ensure that the results are independent of mesh size.

The sample material was assumed to be elastic-plastic with linear elastic behavior up to the yield stress ($\sigma = E\varepsilon$), followed by a power-law type constitutive relation for the post-yield response of the form $\sigma = K\varepsilon^n$, where n is the strain hardening exponent and K is the prefactor that depends on the ratio of modulus to yield strength (E/Y). Von Mises yield criteria with isotropic hardening and rate independent power-law type plastic flow was assumed. In order to cover a wide

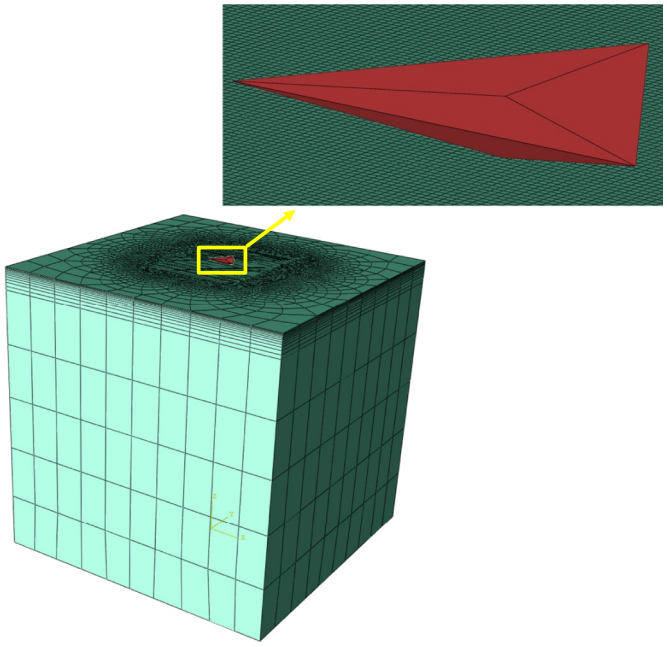

Fig. 1. Full 3D finite element mesh along with the zoomed view of the Berkovich tip and the fine mesh region near the contact.

spectrum of material properties (E/Y) and strain hardening exponent (n) was varied in the range of 10–3000 and 0–0.5, respectively. In all, 130 simulations of sequential indentations were carried out for the different material and spacing combinations. Hardness was calculated for each indent using the load and contact area output (CAREA) obtained directly from ABAQUS which is the most accurate measure of contact area and is not affected by pile-up/sink-in or any geometric effects of surrounding indents, especially when the indents physically overlap.

3. Results and discussion

3.1. Effect of indentation spacing on hardness and elastic modulus

Fig. 2 shows the mean hardness and elastic modulus of indentation tests on fused silica using a Berkovich indenter at different normalized spacing. The mean and standard deviation are calculated from an indentation array of 1225 indents. It was found that the data is normally distributed and hence the mean and standard deviations are appropriate metrics for further analysis. It can be clearly observed from the plot that the hardness and elastic modulus do not show any significant change beyond a normalized spacing of 5. Interestingly, this is less than the diagonal to depth ratio for a Berkovich indenter which is 6.5. For normalized spacing less than 5, the hardness and elastic modulus decreases and even at a normalized spacing of 3 wherein the indents geometrically overlap significantly, the deviation in hardness is not more than 10% and in the case of modulus it is less than 5%. The deviation in modulus being less than that of hardness at a given normalized spacing can be reconciled by the fact that the modulus is a material property that is not significantly affected by the residual strain field of the neighboring indent unless the indents geometrically overlap.

In order to assess the extent of deviation in hardness or modulus with spacing, hardness and modulus are normalized by the corresponding value at a normalized spacing of 20 which represents an extreme case and meets the commonly followed criteria of indent spacing being at least 3 times the lateral dimension of the indent. Fig. 3a shows the normalized mean hardness as a function of normalized spacing for all the bulk materials studied as a part of this work. It can be observed from the plot that the deviation in hardness is insignificant for any material above a normalized spacing of 10 which is less than half of the commonly followed criteria of spacing the indents at least 3 times the lateral dimension of the indent.

Fig. 4 shows optical micrographs of the indentation arrays in aluminum at normalized spacing of 5, 10 and 20. A normalized spacing of 20 is the current standard for minimum indentation spacing where the indents are widely spaced (Fig. 4c), while the current work shows that a normalized spacing of 10 is sufficient to accurately measure hardness and modulus even though the indents are just separated as shown in Fig. 4b. At a normalized spacing of 5 (Fig. 4a), the indents overlap and result in significant hardness deviation. Even at a normalized spacing of 8, which is the minimum spacing that ensures than the indents do not geometrically overlap for the case of a Berkovich geometry, the deviation in hardness is not more than 10% for all the materials shown in Fig. 3. Interestingly, normalized hardness for normalized spacing less than 10, can either increase or decrease depending on the material. Similar trend is observed in the case of modulus, although the deviations are slightly less at a given normalized spacing compared to hardness, as shown in Fig. 3b.

Fig. 5 shows the normalized hardness as a function of the normalized spacing calculated from the finite element simulations for the wide material spectrum mentioned earlier. The FEA calculations clearly show that the hardness deviation is insignificant beyond a normalized spacing of 10, which agrees well with the experimental observations. Similar to the experimental observations, for normalized spacing less than 10, the normalized hardness can either increase or decrease depending on the material property. However, a close look at the plot indicates that the normalized hardness increases in the case of materials that show significant strain hardening capability. This is due to that fact that strain hardening results in an increase in flow stress (strength) in the plastic zone of the residual indent that leads to increased hardness for the

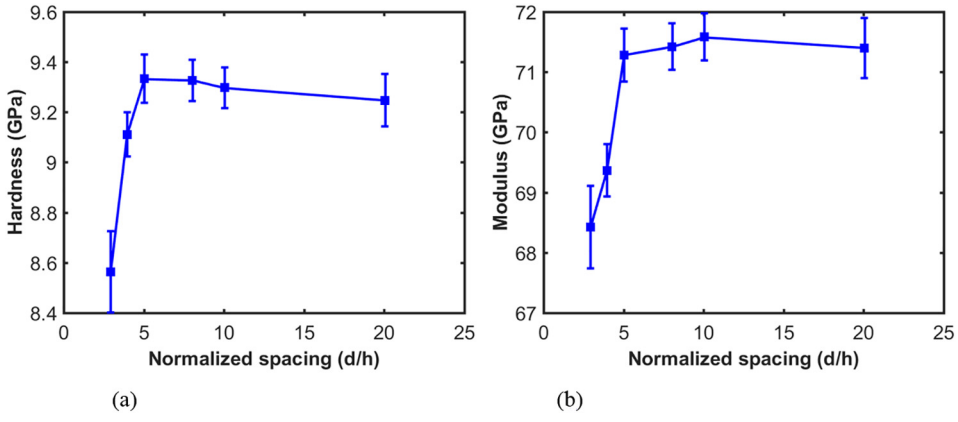

Fig. 2. Experimentally determined (a) hardness and (b) elastic modulus of fused silica at different normalized indent spacing.

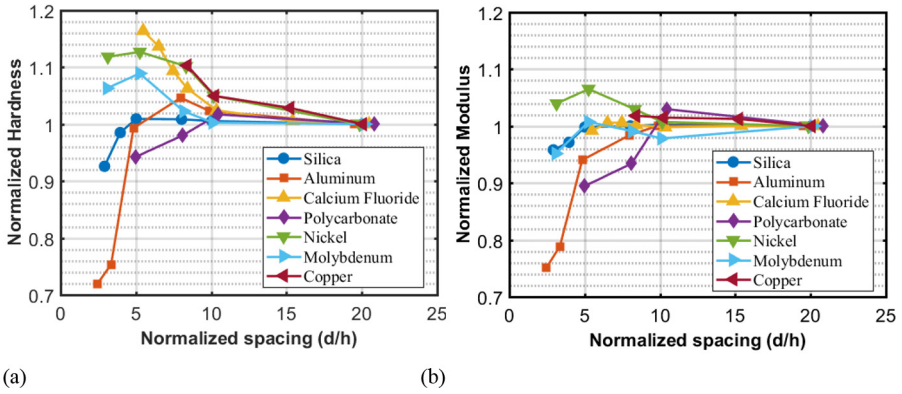

Fig. 3. Experimentally determined (a) normalized hardness and (b) normalized modulus as a function of normalized spacing for the different bulk materials tested in the present study.

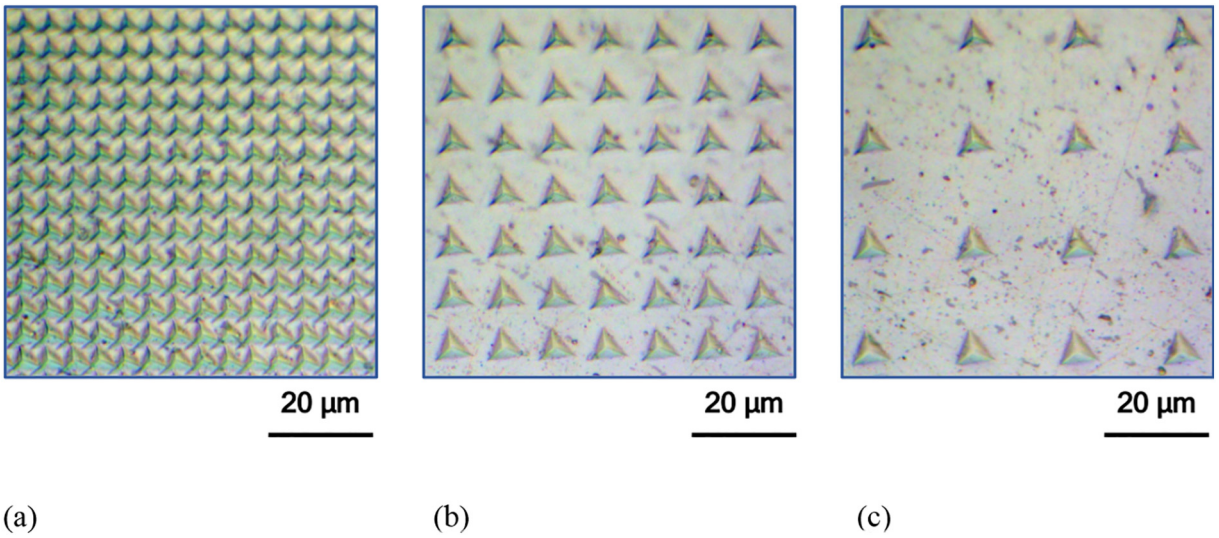

Fig. 4. Optical micrographs of indentation arrays at normalized spacing of (a) 5, (b) 10 and (c) 20 in aluminum.

subsequent indent if the plastic zones overlap. This aspect will be discussed in detail in the next section. At normalized spacing less than 8 for a Berkovich indenter, the residual impression of the indents overlap and the observed hardness can have significant contribution from the geometric effects in addition to the material property effects. In order to distinguish between the material effects and geometric effects, the normalized hardness from FEA at different normalized spacings is plotted in Fig. 6, as a function of a material parameter $(E/Y)^n$ which incorporates all the input parameters of the constitutive relation chosen in the present study. The plot shows that the normalized hardness is almost independent of the material parameter $(E/Y)^n$ for normalized spacing greater than or equal to 10 and shows an increasing trend with the chosen parameters for spacings less than 8. This indicates that material effects are important only in the regime where geometric effects come into play, which is at normalized spacing of less than 8 for a Berkovich indenter and under such conditions the material effects approximately scale with $(E/Y)^n$. This is to be expected as material with higher strain hardening capability results in an increase in flow stress (strength) in the plastic zone of the residual indent that leads to increased hardness for the subsequent indent if the plastic zones overlap.

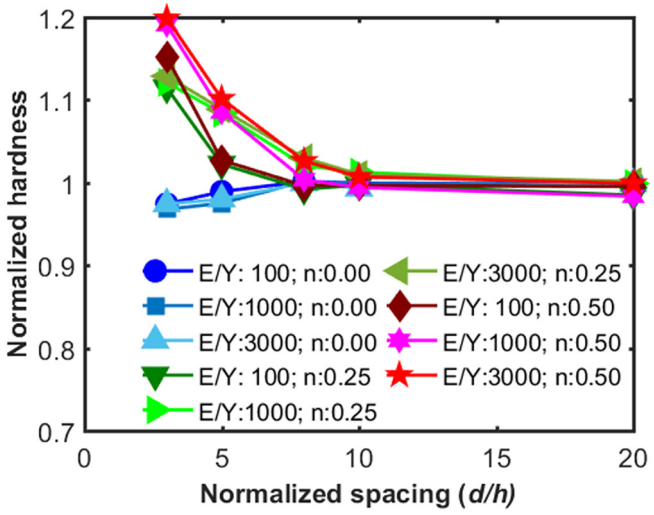

Fig. 5. FEA calculations of normalized hardness as a function of normalized spacing for materials having different E/Y and n.

3.2. Plastic zone size

In the previous section, variation in normalized hardness as a function of normalized spacing was presented and the results clearly demonstrate that the deviation in hardness is insignificant for any material beyond a normalized spacing of 10, which is rather surprising as it is significantly less than the criteria used for minimum spacing of indents which was formulated based on the concept of non-overlapping plastic strain zones [8]. To reconcile the findings of the current experimental

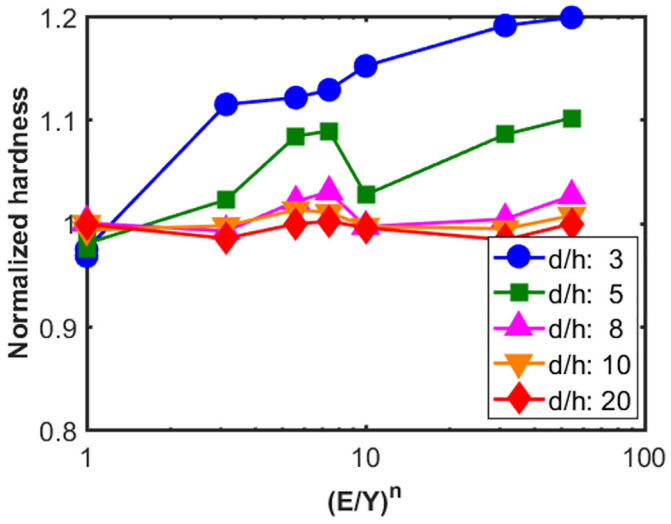

Fig. 6. FEA calculations of normalized hardness as a function of the material parameter $(E/Y)^n$ at different normalized indent spacing for a material with E/Y: 3000 and n: 0.5.

work, the plastic zone underneath the indents obtained from finite element simulations of two sequential indents for a range of normalized spacing (3, 5, 8, 10 and 20) is presented for a material with E/Y of 3000 and n of 0.5, which represents an extreme case of a soft material with high strain hardening capability.

Fig. 7 shows the topographic maps of the indents in the top view and the cross-sectional view of the plastic strain contours to visualize the plastic zone size on a cutting plane that goes from the middle of a face to the opposite edge. The topographic maps show that at a normalized spacing of 3 and 5 the indents geometrically overlap. Even in the case of the indent at a normalized spacing of 8, the indents appear to be well separated due to the scale of the topography map as it can be observed from the cross-sectional images that the indents are just separated. The plastic strain contours underneath the indent at different normalized spacings are shown next to the topography maps at the different normalized spacings. The boundary of the plastic zone is assumed to correspond to a plastic strain of 0.2% to obtain a realistic estimate of the plastic zone size and strains below this are grayed out. From the figure it is very clear that the plastic zones overlap at all the spacings, although they are very minimal at a spacing of 20. The percent deviation in hardness due to spacing calculated from the normalized hardness is indicated next to the plastic zone. Comparison of the plastic zone size and the hardness deviation at a spacing of 10 shows that, in spite of the plastic zones overlapping significantly, the deviation in hardness is less than a few percent. This is rather surprising, as this result is in complete contrast to the commonly believed notion of non-overlapping plastic zones for determining minimum indent spacing.

Given that the plastic zone argument does not stand, a possible alternative explanation for the rather surprising new result could be offered by defining a normalized strength parameter ($\sigma_N = \frac{\sigma_f}{Y}$) which is the ratio of the flow stress to the yield strength. This parameter indicates the extent to which the strength of the material has increased at a particular location due to the plastic strain field of the indent. Fig. 8 shows a contour plot of the equivalent plastic strain and the corresponding normalized strength at a normalized spacing of 10 for two materials having a similar value of E/Y of 3000 but significantly different value of strain hardening exponent n, i.e., $n = 0$ and 0.5. The plastic strain contours for the material with no strain hardening ($n = 0$) is very localized as

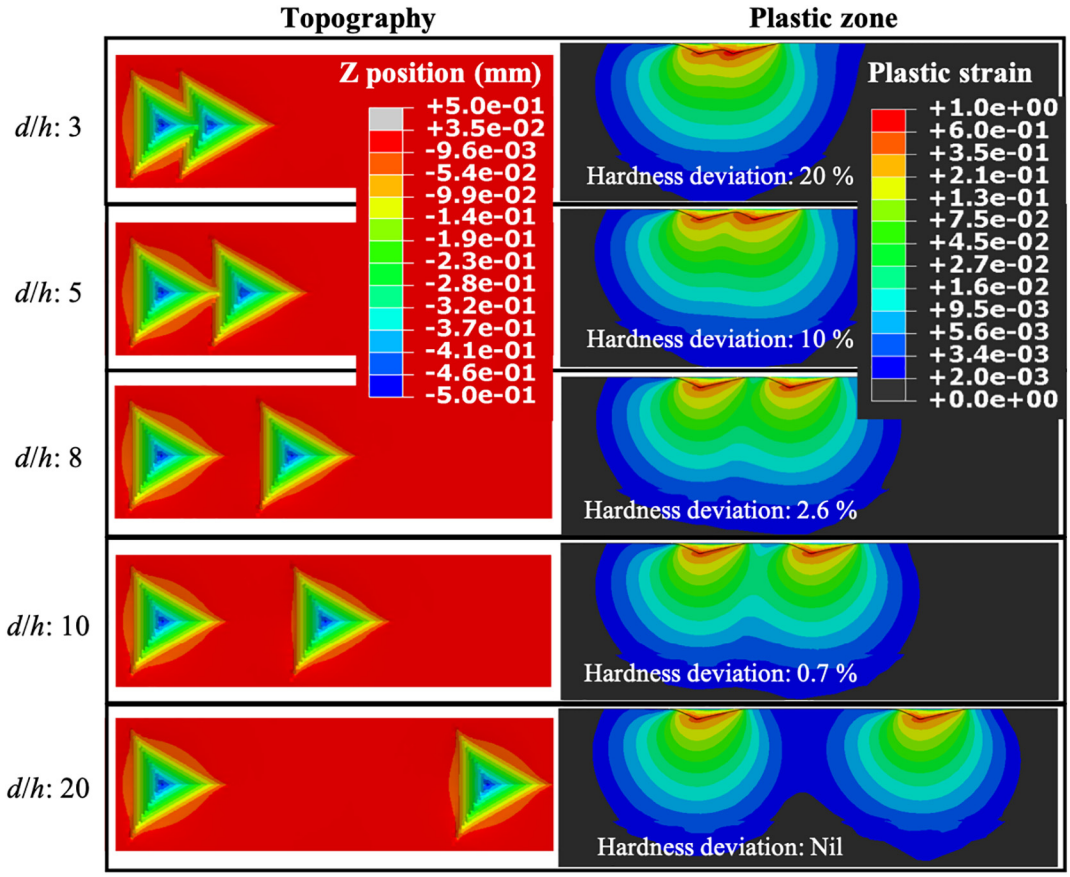

Fig. 7. FEA calculations of indent topography and the cross-sectional plastic strain contours at different normalized spacing for a material with E/Y: 3000 and n: 0.5. Plastic strains below 0.2% are grayed out to visualize the plastic zone boundary.

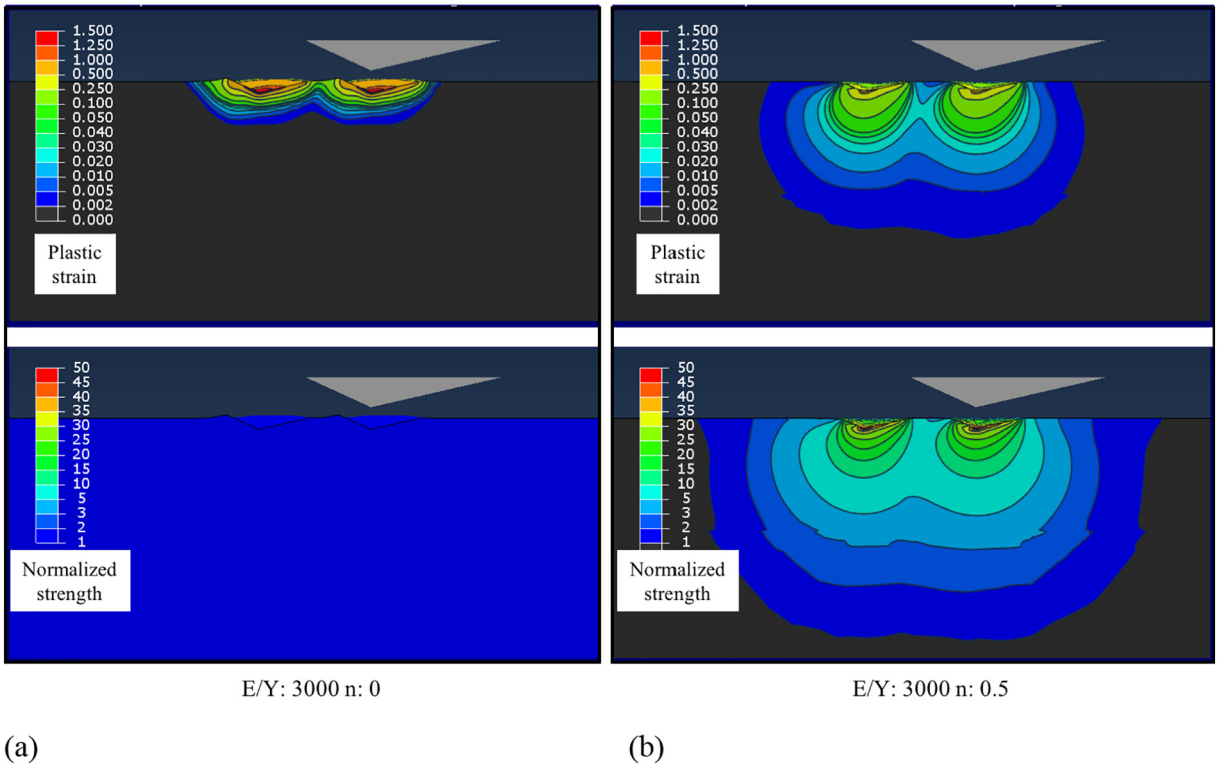

Fig. 8. FEA calculations of plastic strain and normalized strength contours for a material with (a) *E*/*Y*: 3000 and *n*: 0 and (b) *E*/*Y*: 3000 and *n*: 0.5.

expected, while it extends much beyond the contact for the material with significant strain hardening ($n = 0.5$). For both the materials, the plastic zones overlap. For the material with $n = 0$, the normalized strength is uniform everywhere with a value of 1 due to lack of hardening, while the corresponding strength contours for the material with $n = 0.5$, shows significant gradient with values as high as 50 very close to the contact, quickly reducing to less than 10 just outside the contact and eventually reaching a value of 1 at the plastic zone boundary. From simple energy arguments it can be shown that the most of the indentation work (product of hardness and indentation volume) is expended as plastic work ($\int \sigma_f \, d\varepsilon$) in the hemispherical region confined within the contact due to the very high value of the normalized strength and hence the energy contribution of the deformation outside the contact is not significant, thereby resulting in a hardness deviation of less than a few percent for the material with $n = 0.5$ and almost insignificant deviation for the material with strain hardening exponent of $n = 0$. In summary, contrary to the well accepted practice of spacing the indents based on the plastic zone size, which is a strain-based criterion, this work shows that the minimum spacing is determined based on strength distribution that resulted from the deformation produced by the neighboring indent.

3.3. Effect of number of neighboring indents

The results shown in Figs. 2 to 5 focus on the indent spacing effect without regard to the number of neighbors. While the spacing effect is of primary focus in this work, it is also instructive to determine if there is any systematic effect of the number of neighboring indents on the measured hardness at a given normalized spacing. This has important implications for interpreting results from two dimensional arrays which are commonly used for mapping, as the sequence of indents determines the number of neighboring indents and any systematic effect of number of neighbors can potentially lead to erroneous results.

Fig. 9 shows the experimental results of hardness as a function of number of neighboring indents for fused silica at different normalized spacings. The plot clearly shows that the hardness at a given normalized spacing is almost independent of the number of neighbors for normalized spacing greater than 5 and the variation in hardness due to spacing dominates the overall response. Similar behavior is observed for other materials studied in the work. This implies that the sequence of indents in a two-dimensional indentation array does not affect the measured hardness as long as the normalized spacing is greater than or equal to 10.

To further explore the effect of number of neighbors, FEA results for a sequence of 5 indents at a normalized spacing of 10 is shown in Fig. 10 for a material with *E*/*Y* of 3000 and *n* of 0.5. The figure shows topographic contours (Fig. 10a) for the indents and the number next to the indent indicates the sequence of the indent. The indent sequence is chosen such that it mimics most commonly followed experimental sequence of performing indents along rows or columns. This sequence of 5 indents results in indents with 1, 2 and 4 neighbors. The

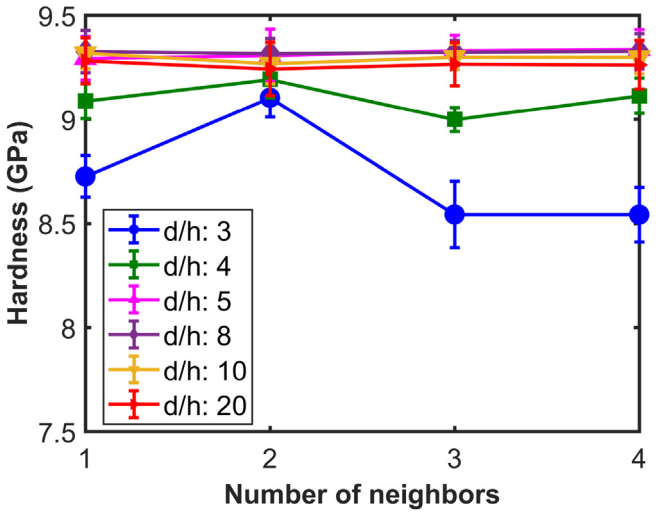

Fig. 9. Experimentally determined hardness as a function of number of neighboring indents at different normalized indent spacing for fused silica.

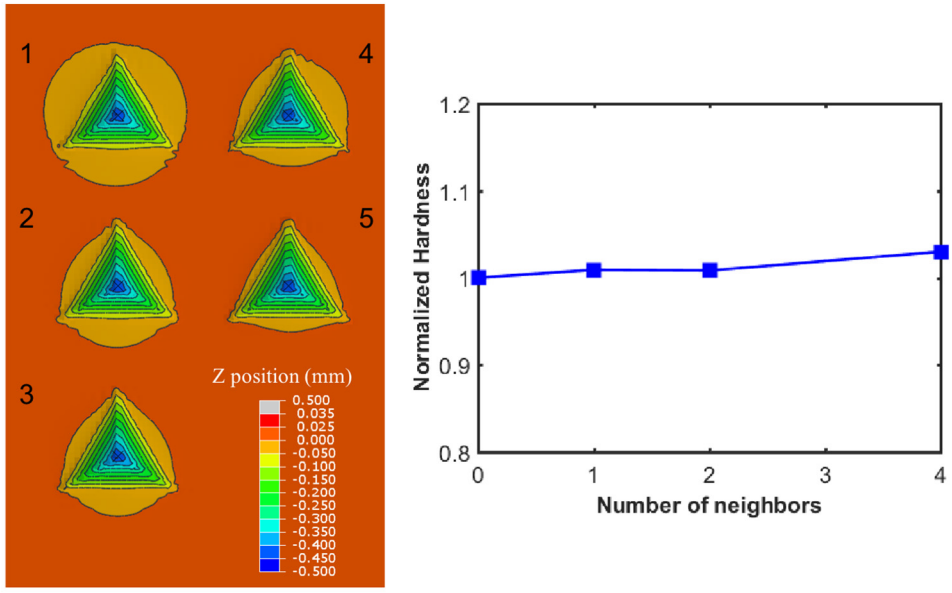

(a) (b)

Fig. 10. (a) FEA results of indent topography for a sequence of 5 indents for a material with E/Y: 3000 and n: 0.5 at a normalized spacing of 10. The sequence of indent is mentioned next to the topographic contour and (b) normalized hardness as a function of number of neighboring indents.

corresponding normalized hardness as a function of number of neighbors is shown in Fig. 10b. While there are obvious differences in the topography of the indents with pile up/sink-in clearly being reduced along the direction of the neighboring indent, the resulting deviation in hardness is not very significant. This result is a natural extension of the results from the previous section, wherein overlapping plastic zones did not necessarily result in significant deviation in hardness as the topographic features or plastic strain fields outside the contact region do not alter the measured hardness significantly.

3.4. Effect of indenter orientation

All the results presented earlier are for a fixed orientation of the three-sided pyramidal indenter and due to the 6-fold symmetry there are multiple possibilities for the indenter orientation. In order to explore the effect of orientation, hardness measured from two different extreme orientations for a Berkovich tip in a sequence of two indents is shown in Fig. 11, for a material with E/Y of 3000 and n of 0.5. The schematic of the indenter orientations along with the indent number is also shown in the figure. It can be observed from the plot that the hardness deviation between the two orientations is insignificant compared to the deviation due to the spacing. This result has implications for indentation mapping as it clearly demonstrates that there is no requirement for aligning the indenter for mapping, which greatly minimizes the experimental effort to align the indenter along any preferential mapping direction.

3.5. Effect of indenter angle

All the results presented up to this point are for a standard Berkovich tip geometry, wherein the centerline to face angle is 65.3°. In order to extend the results to other tip geometries, finite element simulations for two other 3-sided pyramidal tip geometries with centerline to face angle of 55 and 45° are performed.

Fig. 12a shows a comparison of the normalized hardness as a function of normalized spacing for three different three-sided tip geometries for a material with E/Y of 3000 and n of 0.5. The plot shows that the normalized hardness at a given normalized spacing decreases with decreasing indenter angle, which is to be expected as the sharper indenter angles result in smaller residual impression for a given depth. In order to better compare the results across indenter angles, the indent spacing can be normalized by the lateral dimension of the indent which is the distance between the edge and opposite face of the triangular impression (median of the triangle). Fig. 12b shows the normalized hardness as a function of the ratio of indent spacing to median length of the triangular impression. Interestingly, the data from all the indenter angles lie on one master curve, which clearly indicates that the conclusions drawn from the results for the Berkovich indenter can be readily extended to the other indenter angles. The plot also shows that above a normalized spacing of around 1.5, the deviation in hardness is less than a few percent, which may not be experimentally distinguishable and reinforces the conclusion drawn earlier that the minimum spacing of indents need not be three times the lateral dimension of the indent, for any indenter angle which by logical extension applies to a spherical indenter as well. Furthermore, even at a normalized spacing of 1, which is the minimum spacing required to ensure that the indents do not geometrically overlap, the deviation in hardness is only 5% for the extreme case of the material property chosen (E/Y: 3000 and n: 0.5). This also reinforces the argument that for any indenter geometry, the majority of the input indentation work is expended in a hemispherical region within the contact.

3.6. Extension to film on substrate systems

In this section, we present the effect of the indent spacing on the hardness of film-on-substrate system, which has additional complication of gradient in properties compared to bulk materials. For this study, a soft film on hard substrate system (200 nm gold film on silica substrate) is chosen as it shows significant pile-up and serves as an extreme case for the spacing study. In the case of film on substrate systems, film thickness is an additional length scale that needs to be considered in the analysis and results at a fixed value of the ratio of indentation depth to film thickness (h/t) can be compared across different spacings. Also, indents performed to different values of h/t, conveniently result in exploring the spacing effect over a range of material properties, starting from film dominated properties to substrate dominate properties with increasing h/t.

Fig. 13a shows the normalized hardness as a function of normalized spacing for indents performed to different values of h/t. At higher values

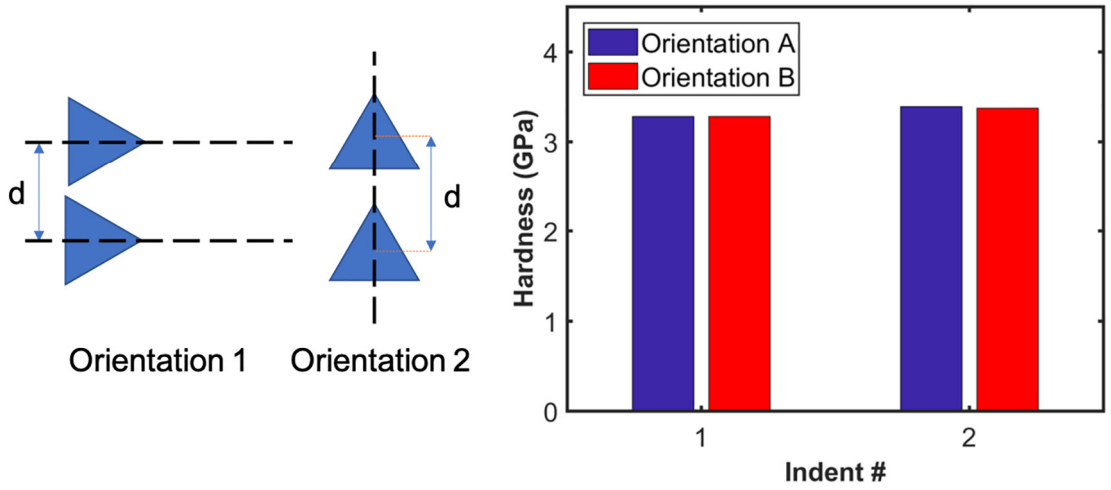

Fig. 11. FEA calculations of the orientation dependence of hardness for two sequential indents on a material with E/Y: 3000 and n: 0.5 at a normalized spacing of 8.

of h/t (1 and 3), where the response is dominated by the silica substrate, hardness does not show significant deviation with spacing even at small spacings. However, at smaller values of h/t (0.25 and 0.5), the contribution of the gold film is significant and the normalized hardness shows a decreasing trend below a normalized spacing of 10. These results are similar to those for bulk materials wherein a normalized spacing of 10 was found to be sufficient to obtain accurate results. To further demonstrate the significance of this result, Fig. 13b shows a topographic map along with a depth profile at the location shown in the map for a few indents at h/t of 1 and a normalized spacing of 10. The profile shows that the pile-up is comparable to the indentation depth which is an extreme case that occurs mostly for soft films on hard substrates and even for such extreme cases a normalized indent spacing of 10 is sufficient to obtain reliable results. This clearly demonstrates that a normalized spacing of 10 for a Berkovich tip is sufficient to obtain reliable results for any combination of material properties and film on substrate systems.

4. Implications for design

The significant reduction in the minimum indent spacing observed in the present work has major implications for high speed nanoindentation testing and opens up an opportunity to measure the local mechanical properties with much higher resolution by large arrays of indents [7], which, in turn, serves as an effective characterization tool to significantly reduce design and production time [3]. For example, this could also be particularly useful for studying the processing induced gradients in mechanical properties commonly encountered in additively manufactured components which is currently a prime area of materials research. A quick but exhaustive study of the local mechanical properties coupled with microstructural investigations for various build strategies would be a significant contribution to the field. Furthermore, accurately measuring the local mechanical properties is of immense value for developing complex thermal barrier coatings, extensively employed in gas turbines, wherein, recent reports have suggested coupling nanoindentation mapping data with tomographic imaging to predict the properties of the coatings using Object Oriented Finite element analysis (OOF) [16]. High-resolution mechanical property maps can be deconvoluted to accurately determine the properties of the individual phases which can in turn be used as inputs for FEA. This would be a major step in embracing an integrated computational materials engineering (ICME) approach, which aims to effectively integrate modeling and experiments to enable materials development [17].

5. Summary and conclusions

(i) Extensive indentation testing and finite element analysis has been carried out at different indent spacings for a wide variety of materials to critically assess the commonly followed minimum indent spacing criteria.

(ii) A minimum indent spacing of 10 times the indentation depth was found to result in insignificant deviation in hardness for all the bulk materials and coatings tested in this work using a Berkovich

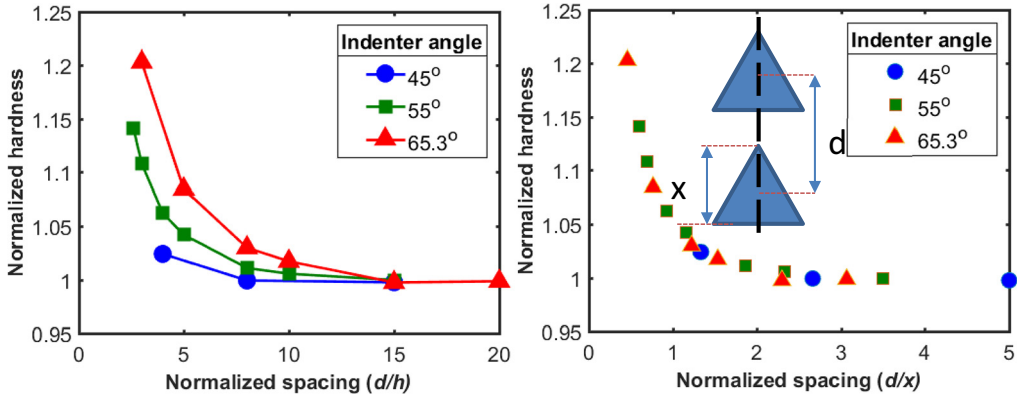

Fig. 12. FEA calculations of normalized hardness as a function of (a) ratio of indent spacing to indent depth and (b) ratio of indent spacing to the lateral dimension of the indent for three different 3-sided pyramidal indenters for a material with E/Y: 3000 and n: 0.5.

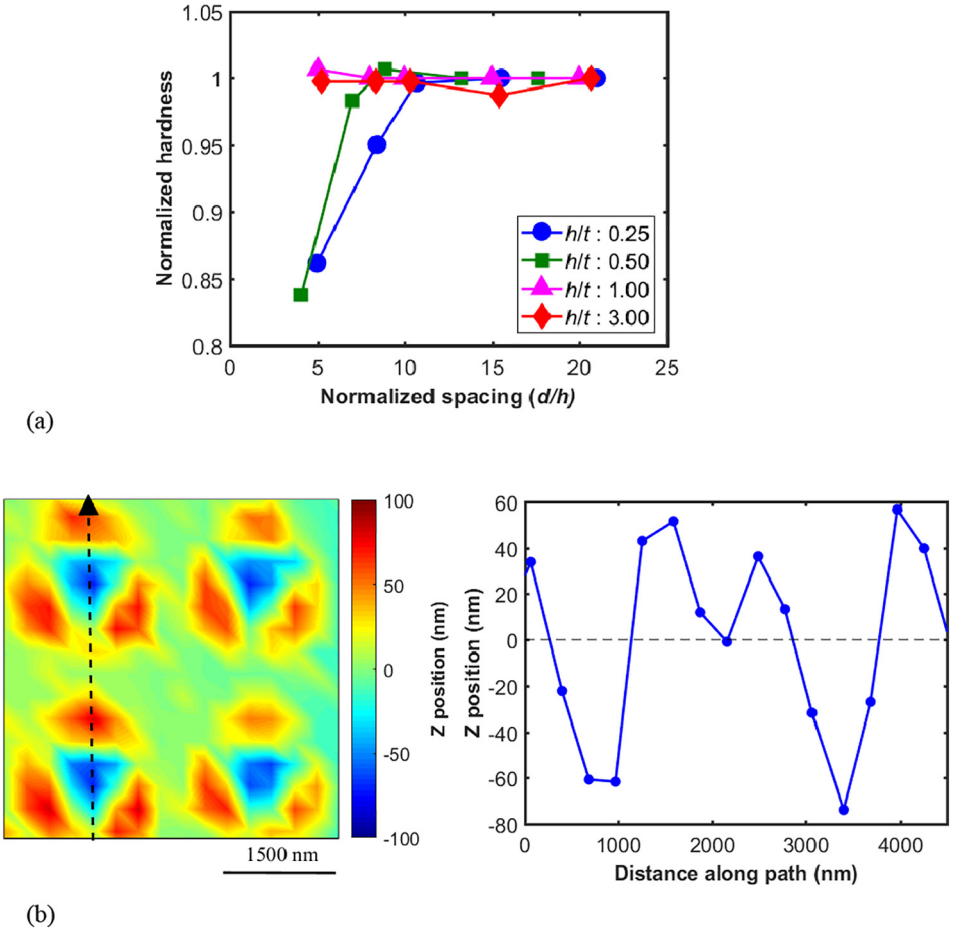

Fig. 13. (a) Experimentally determined normalized hardness as a function of normalized spacing at different ratios of depth to film thickness for gold film on silica substrate and (b) topographic map and the depth profile along the path shown in the topographic map for a region in the indent array at a depth to film thickness ratio of 1 and spacing to depth ratio of 10.

indenter. This is less than half of the commonly followed criteria of spacing the indents three times the lateral dimension of the indent, which for a Berkovich indenter is approximately 20 times the indent depth.

(iii) The observed minimum spacing criteria was rationalized by the fact that the majority of the input indentation energy is expended in plastic deformation within a hemispherical region bounded by the contact zone, where the normalized strength (ratio of flow stress to yield strength) is very high.

(iv) Contrary to the well accepted practice of spacing the indents based on the plastic zone size, which is a strain-based criterion, this work shows that the minimum spacing is determined based on strength distribution that resulted from the deformation produced by the neighboring indent.

(v) The minimum indent spacing criteria was also studied for different 3-sided pyramidal tip geometries. It was found that the hardness deviation for different indenter angles falls on a master curve for a given material, and a minimum indent spacing of 1.5 times the indent contact lateral dimension is sufficient to obtain accurate results. By logical extension, these results are also applicable to spherical and Vickers geometry.

(vi) The effect of indent orientation and the number of neighboring indents was found to be less significant compared to the spacing effect, which demonstrates that there is no specific requirement for aligning the indenter during mapping, there by greatly minimizing the experimental effort involved in aligning the indenter.

(vii) These results have significant ramifications for indentation mapping wherein the indents can now be placed much closer than what was traditionally accepted, which enables high resolution mechanical property mapping and serves as an effective characterization tool to significantly reduce design and production time.

Data availability

The raw/processed data required to reproduce these findings cannot be shared at this time due to technical or time limitations.

References

[1] D. Tabor, The Hardness of Metals, Clarendon, Oxford, 1951.
[2] W.C. Oliver, G.M. Pharr, An improved technique for determining hardness and elastic modulus using load and displacement sensing indentation experiments, J. Mater. Res. 7 (1992) 1564–1583, https://doi.org/10.1557/JMR.1992.1564.
[3] E.P. Koumoulos, S.A.M. Tofail, C. Silien, D. De Felicis, R. Moscatelli, D.A. Dragatogiannis, E. Bemporad, M. Sebastiani, C.A. Charitidis, Metrology and nanomechanical tests for nano-manufacturing and nano-bio interface: challenges & future perspectives, Mater. Des. 137 (2018) 446–462, https://doi.org/10.1016/j.matdes.2017.10.035.
[4] N.X. Randall, M. Vandamme, F.J. Ulm, Nanoindentation analysis as a two-dimensional tool for mapping the mechanical properties of complex surfaces, J. Mater. Res. 24 (2009) 679–690, https://doi.org/10.1557/jmr.2009.0149.
[5] M. Sebastiani, R. Moscatelli, F. Ridi, P. Baglioni, F. Carassiti, High-resolution high-speed nanoindentation mapping of cement pastes: unravelling the effect of microstructure on the mechanical properties of hydrated phases, Mater. Des. 97 (2016) 372–380, https://doi.org/10.1016/j.matdes.2016.02.087.
[6] E.D. Hintsala, U. Hangen, D.D. Stauffer, High-throughput nanoindentation for statistical and spatial property determination, JOM 70 (2018) 494–503, https://doi.org/10.1007/s11837-018-2752-0.
[7] J.J. Roa, P. Sudharshan Phani, W.C. Oliver, L. Llanes, Mapping of mechanical properties at microstructural length scale in WC-Co cemented carbides: assessment of

hardness and elastic modulus by means of high speed massive nanoindentation and statistical analysis, Int. J. Refract. Met. Hard Mater. 75 (2018) 211–217, https://doi.org/10.1016/j.ijrmhm.2018.04.019.
[8] L. Samuels, T.O. Mulhearn, An experimental investigation of the deformed zone associated with indentation hardness impressions, J. Mech. Phys. Solids 5 (1957) 125–134, https://doi.org/10.1016/0022-5096(57)90056-X.
[9] ASTM E384, Standard Test Method for Knoop and Vickers Hardness of Materials, ASTM Int., 2016 1–28, https://doi.org/10.1520/E0384-11E01.2.
[10] ASTM E92, Standarad Test Methods for Vickers Hardness and Knoop Hardness of Metallic Materials, ASTM Int., 2017https://doi.org/10.1520/E0092-17.
[11] ASTM E18, Standard Test Methods for Rockwell Hardness of Metallic Materials, ASTM Int., 2018https://doi.org/10.1520/E0018-18A.
[12] ASTM C1327, Standard Test Method for Vickers Indentation Hardness of Advanced Ceramics, ASTM Int., 2015https://doi.org/10.1520/C1327-15.
[13] ISO-14577, Metallic Materials–Instrumented Indentation Test for Hardness and Materials Parameters, ISO Central Secretariat Geneva, Switzerland, 2002.
[14] ISO-6507-1, Metallic Materials—Vickers Hardness Test, ISO Central Secretariat Geneva, Switzerland, 2005.
[15] P. Sudharshan Phani, W.C. Oliver, Ultra high strain rate nanoindentation testing, Materials (Basel) 10 (2017) 663–674, https://doi.org/10.3390/ma10060663.
[16] R. Vaßen, Y. Kagawa, R. Subramanian, P. Zombo, D. Zhu, Testing and evaluation of thermal-barrier coatings, MRS Bull. 37 (2012) 911–916, https://doi.org/10.1557/mrs.2012.235.
[17] C.G. Levi, J.W. Hutchinson, M.-H. Vidal-Sétif, C.A. Johnson, Environmental degradation of thermal-barrier coatings by molten deposits, MRS Bull. 37 (2012) 932–941, https://doi.org/10.1557/mrs.2012.230.